Systematic Identification of Lysine 2-hydroxyisobutyrylated Proteins in *Proteus mirabilis*[*][S]

Hanyang Dong‡, Zhenchang Guo‡§, Wei Feng¶, Tao Zhang¶, Guijin Zhai‡, Agata Palusiak‖, Antoni Rozalski‖**, Shanshan Tian‡, Xue Bai‡, Lijin Shen‡, Pu Chen‡, Quan Wang§, Enguo Fan‡‡, Zhongyi Cheng§§, and Kai Zhang‡¶¶**

Lysine 2-hydroxyisobutyrylation (K_{hib}) is a novel post-translational modification (PTM), which was thought to play a role in active gene transcription and cellular proliferation. Here we report a comprehensive identification of K_{hib} in *Proteus mirabilis (P. mirabilis).* By combining affinity enrichment with two-dimensional liquid chromatography and high-resolution mass spectrometry, 4735 2-hydroxyisobutyrylation sites were identified on 1051 proteins in *P. mirabilis.* These proteins bearing modifications were further characterized in abundance, distribution and functions. The interaction networks and domain architectures of these proteins with high confidence were revealed using bioinformatic tools. Our data demonstrate that many 2-hydroxyisobutyrylated proteins are involved in metabolic pathways, such as purine metabolism, pentose phosphate pathway and glycolysis/gluconeogenesis. The extensive distribution of K_{hib} also indicates that the modification may play important influence to bacterial metabolism. The speculation is further supported by the observation that carbon sources can influence the occurrence of K_{hib}. Furthermore, we demonstrate that 2-hydroxyisobutyrylation on K343 was a negative regulatory modification on Enolase (ENO) activity, and molecular docking results indicate the regulatory mechanism that K_{hib} may change the binding formation of ENO and its substrate 2-phospho-D-glycerate (2PG) and cause the substrate far from the active sites of enzyme. We hope this first comprehensive analysis of nonhistone K_{hib} in prokaryotes is valuable for further functional investigation of this modification. *Molecular & Cellular Proteomics 17: 10.1074/mcp.RA117.000430, 482–494, 2018.*

Protein post-translational modifications (PTMs)[1] play key roles in diverse biological processes (1). Lysine acylation have been thought to be one of the most extensive PTMs (2), involving in gene transcription, energy metabolism and signal transduction (3–8). In last five years, the landscape of lysine acylation has been increasingly expanded with improvement of mass spectrometry techniques (9) and pan-antibody enrichment methods (10), and a series of novel lysine modifications have been reported including succinylation (7, 11–15), crotonylation (16–19), malonylation (12, 20, 21), and glutarylation (21–23). To date, these novel lysine PTMs have attracted considerable attention in biomedical field.

Recently lysine 2-hydroxyisobutyrylation (K_{hib}) was reported as a new histone mark in eukaryotic cells (24). In the report, 63 K_{hib} sites were identified on histone proteins and H4K8hib was further considered to regulate gene transcriptional activity (24, 25), furthermore, 2-hydroxyisobutyrylation on histone H4K8 is regulated by glucose homeostasis and H4K8$_{hib}$ can influence proliferation of *Saccharomyces cerevisiae* (26), which indicates that the novel lysine modification may have potential functions in cellular regulations (2, 8).

Accumulating evidence suggests that lysine PTMs are usually distributed in diverse model organisms. For example, many lysine acetylated proteins are involved in the regulation of pathways in both eukaryotes and prokaryotes (13, 27).

---

[1] The abbreviations used are: PTMs, post-translational modifications; Khib, lysine 2-hydroxyisobutyrylation; HibCoA, 2-hydroxyisobutyryl-CoA; UTI, urinary tract infection; 2HIBA, 2-hydroxyisobutyrate; AGC, automatic gain control; FDR, false discovery rate.

Therefore, it is interesting if K_{hib} exists in prokaryotes too? If so, what roles do these discovered K_{hib} play? The knowledge gap should be filled in to improve our understanding of the novel lysine PTM.

In this study, we combined affinity enrichment with two-dimensional LC separation and mass spectrometric analysis to perform a systematic analysis of K_{hib} in *P. mirabilis*, which is one of the most common causes of urinary tract infections (UTI) in individuals with long term indwelling catheters. This work demonstrated that K_{hib} is widely distributed in prokaryotes, for the first time. We identified 4735 2-hydroxy-isobutyrylation sites on 1051 proteins and further character-ized the abundance and localization of the modification in *P. mirabilis*. Bioinformatic analysis demonstrated that these 2-hydroxyisobutyrylated proteins are involved in diverse bio-logical processes and enriched in metabolic pathways. Our data further demonstrated that pyruvate, glucose, and 2-hy-droxyisobutyrate (2-HIBA) influenced 2-hydroxyisobutyryla-tion status of proteins. In addition, molecular docking result indicates that K_{hib} can change the binding conformation of enzyme and its substrate, then cause the substrate far from the active sites of enzyme. Finally, we confirmed 2-hydroxy-isobutyrylation on K343 was a negative regulatory modifica-tion on Enolase (ENO) activity by mutagenesis experiments.

EXPERIMENTAL PROCEDURES

Materials — Anti-2-hydroxyisobutyryl pan antibodies and conjugated-agarose beads were from PTM Biolabs, Inc (Hangzhou, China). Colloidal Blue Staining Kit was from Invit-rogen (Carlsbad, CA) and 2×YT medium and Luria-Bertani (LB) were from Oxoid (Basingstoke, UK). C18 ZipTips and iodoacetamide were from Millipore (Bedford, MA), HisPur Ni-NTA Resin was from Thermo Fisher Scientific (Waltham, MA), Amicon Ultra-0.5 Centrifugal Filter Device was from Millipore (Bedford, MA). *P. mirabilis* strain ATCC29906 was supplied by Dr. Antoni Rozalski and Agata Palusiak from University of Lodz.

Cell Culture, Protein Extraction, and Digestion — *P. mirabilis* strain ATCC29906 was cultured overnight in 2×YT medium at 37 °C and then harvested during the exponential growth phase by centrifugation. Next, ten milligrams of proteins were extracted and the resulting pellet was digested according to a previously described procedure (27). The tryptic peptides were desalted through SepPak C18 cartridges (Waters, Mil-ford, MA) and vacuum-dried before fractionation.

Fraction and Enrichment of 2-hydroxyisobutyryllysine Pep-tides — Tryptic peptides were fractionated using high pH re-versed phase HPLC (L-3000 HPLC System, Rigol) on Waters XBridge Prep C18 column (5 μm particles, 130 Å, 4.6 × 250 mm). Mobile phases A (2% acetonitrile, pH 10.0) and B (98% acetonitrile) were used to develop a gradient elution. The solvent gradient was set as follows: 5–8% B, 4 min; 8–18% B, 16 min; 18–32% B, 30 min; 32–95% B, 3 min; 95% B, 5 min; 95–5% B, 2 min. The tryptic peptides were separated at an

eluent flow rate of 1 ml/min and monitored at 214 nm. The column oven was set as 40 °C. Eluent was collected every minute and marked each component by time. The same tail number marked components were combined into 10 fractions and vacuum-dried for further affinity enrichment.

2-hydroxyisobutyrylated peptides were enriched using agarose-conjugated anti-2-hydroxyisobutyryl lysine antibody. Each fraction of peptides were redissolved in NETN buffer (50 mM Tris-HCl, pH 8.0, 100 mM NaCl, 1 mM EDTA, 0.5% Nonidet P-40), and then incubated with anti- 2-hydroxyisobutyryllysine antibody conjugated protein A agarose beads at 4 °C over-night with gentle rotation. The supernatant was removed and the beads were washed three times with NETN buffer, twice with ETN buffer (50 mM Tris-Cl, pH 8.0, 100 mM NaCl, 1 mM EDTA), followed by three times wash with water. The bound peptides were eluted by washing three times with 1% triflu-oroacetic acid. The eluates were combined and dried. The resulting peptides were cleaned with C18 ZipTips (Millipore Corp.) according to the manufacturer's instructions, prior to nano-HPLC/mass spectrometric analysis.

HPLC-MS/MS Analysis — Each sample of enriched K_{hib} peptides was reconstituted in 7 μl of HPLC buffer A (0.1% (v/v) formic acid in water), and 5 μl was injected into a Nano-LC system (EASY-nLC 1000, Thermo Fisher Scien-tific, Waltham, MA). Each sample was separated by a C18 column (50 μm inner-diameter × 15 cm, 2 μm C18) with a 125 min HPLC-gradient (linear gradient from 2 to 35% HPLC buffer B (0.1% formic acid in acetonitrile) in 110 min, and then to 90% buffer B in 15 min). The HPLC elute was electros-prayed directly into an Orbitrap Q-Exactive mass spectrom-eter (Thermo Fisher Scientific, Waltham, MA). The source was operated at 2.4 kV. The mass spectrometric analysis was carried out in a data-dependent mode with an automatic switch between a full MS scan and an MS/MS scan in the orbitrap. For full MS survey scan, automatic gain control (AGC) target was 3e6, scan range was from 350 to 1800 with the resolution of 70,000. The 15 most intense peaks with charge state 2 and above were selected for fragmentation by higher-energy collision dissociation (HCD) with normalized collision energy of 27%. The MS2 spectra were acquired with 17,500 resolution. The exclusion duration for the data-depen-dant scan was 15 s, the repeat count was 2, and the exclusion window was set at 2.2 Da.

Database Search and Verification of 2-hydroxyisobutyry-lated Peptides — The resulting MS/MS data were searched against UniProt *P. mirabilis* ATCC 29906 database (3812 pro-teins, downloaded April 28, 2016) using MaxQuant software (v1.5.2.8) with false discovery rate (FDR) for protein, peptide and modification of less than 1%. Peptide sequences were searched using trypsin specificity and allowing a maximum of two missed cleavages. The minimal peptide length was set to seven. Carbamidomethylation on Cys was specified as fixed modification. 2-hydroxyisobutyryl on lysine, oxidation of me-thionine and acetylation on peptide N-terminal were fixed as
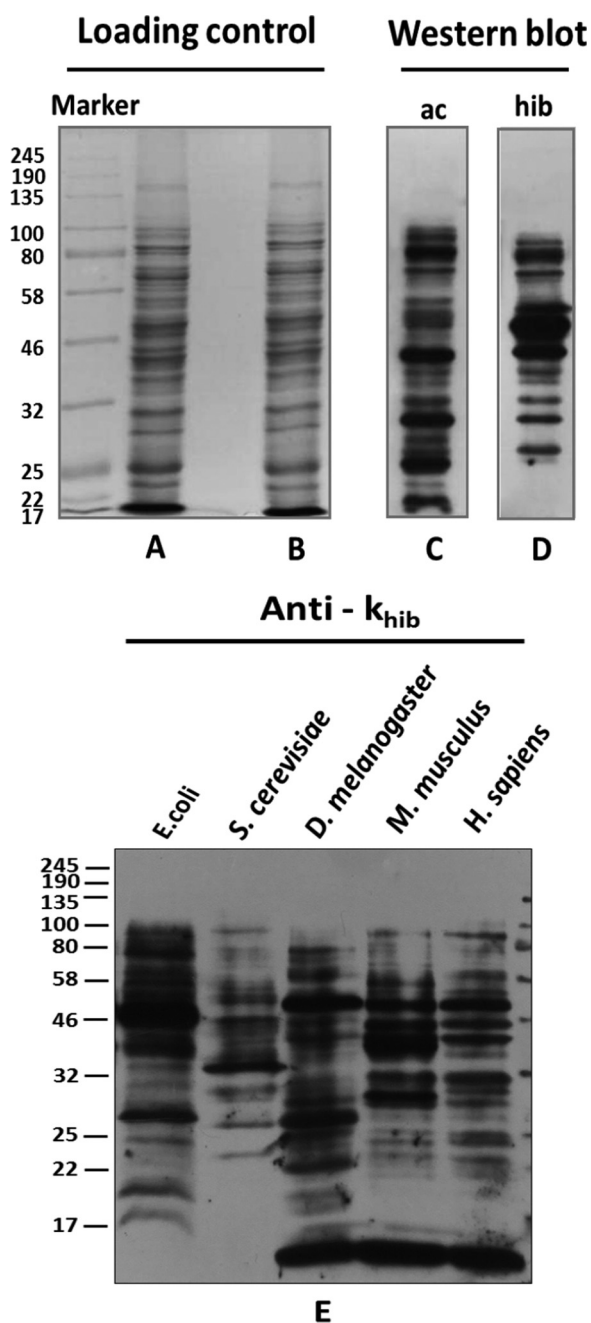
Fig. 1. Detection of lysine 2-hydroxyisobutyrylation and lysine acetylation by Western blot analysis. SDS-PAGE gel stained with Colloidal Blue as the loading control. *A*, whole-cell lysates from *P. mirabilis* (for C: Anti-acetylation). *B*, whole-cell lysates from *P. mirabilis* (for D: Anti-2-hydroxyisobutyrylation). *C*, anti-acetyllysine antibody for whole-cell lysates from *P. mirabilis*. *D*, anti-2-hydroxy-isobutyrylation antibody for whole-cell lysates from *P. mirabilis*. *E*, anti-2-hydroxyisobutyrylation antibody for whole-cell lysates from *E. coli* (K-12 MG1655), *S. cerevisiae* (strain BJ5464 - npga), *D. melano-gaster* (S2 cells), *M. musculus* (C2C12 cells) and *H. sapiens* (HeLa cells).

variable modifications. Mass tolerances for precursor ions were set at ± 10 ppm for precursor ions and ± 0.02 Da for MS/MS. Identified 2-hydroxyisobutyrylated peptides with

MaxQuant score below than 50, localization probability < 0.75 and PEP > 0.001 were further excluded. The interesting MS/MS spectra were manually verified. To verify the accuracy of the MS/MS result, we prepared the modified peptides and compared the MS/MS spectrum of the *in vivo* peptides with their counterpart synthetic peptides.

Bioinformatics Analysis—Gene Ontology annotation and protein-protein interaction were performed by DAVID and STRING, sequence Logo representations of significant motifs were identified by Motif-X software. Finally, we analyzed the distribution of 2-hydroxyisobutyrylated proteins in metabolic pathways by KEGG Pathway.

Identification of Lysine 2-hydroxyisobutyrylation Substrates— *P. mirabilis* cells were cultured in M9 medium (supplemented with each of the 20 amino acids at 100 mg/l) or M9 medium supplemented with 0.8% pyruvate, 0.8% glucose, or 0.8% 2-HIBA, respectively. The cells were harvested after 36 h, lysed, and Western blotted with pan-antibodies against 2-hy-droxyisobutyryllysine. Coomassie Blue staining was used for the loading controls.

Simulation of Binding of Substrate and Enzymes—Auto-Dock 4.0 was used to dock small molecules (substrates) into their enzyme structures with and without K_{hib}, respectively (28). The original enzyme structure was predicted using Swiss model server (29). The enzymatic structure with K_{hib} was generated by modifying the side chain of lysine using Chimera software (30). The structure of small molecules was download from DrugBank (31). In this study, small molecule—2-phos-pho-D-glycerate (2PG) and the corresponding enzyme—eno-lase (ENO) were selected as example. The information on active sites and substrate binding sites of ENO was obtained from UniProt database (32). Before the docking simulation, the small molecule was placed into the substrate binding site of enzyme as the start point of docking. The parameters for docking were set as follows: the Lamarckian genetic algo-rithm (LGA) runs were set at 50, and the maximum number of energy evaluations was set at 2.5 million. The simulation box was fixed at the center of the substrate and the box size was set at 60 Å$\times$60 Å$\times$68 Å in all three dimensions. The confor-mation with the highest binding energy of small molecule was considered as the enzyme-bound conformation. By compar-ing the binding energy and position between the enzymatic structure with and without K_{hib}, we infer the likely effect of such modification on enzymatic activity.

Site-directed Mutagenesis and Purification of ENO—First, we structured pET28a-ENO vector for expression, we used this primers to clone ENO gene: ENO-sense: 5′-CGCGGAT-CCTCCAAAATCGTTAAAG-3′, ENO-antisense: 5′-CCGCTC-GAGTTATGC TTGGCCTTTAACTTC-3′, and selected BamHI and XhoI as restriction enzyme cutting sites to insert ENO into pET28a, the constructed vectors were transformed into *E. coli* BL21 (DE3) for protein expression. Next, the mutated sites of ENO gene were introduced into the pET28a-ENO by PCR reaction, and the primers were given below: K343T-sense:
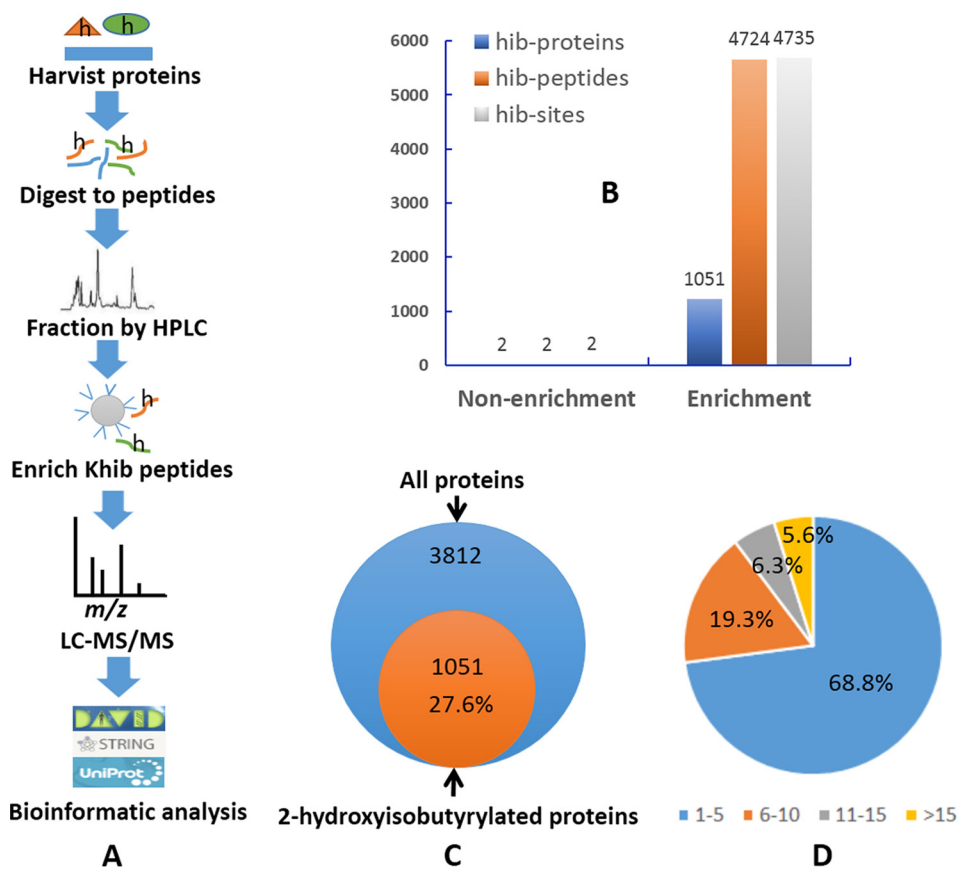
FIG. 2. **Profiling K$_{hib}$ in *P. mirabilis*.** *A,* The analytical strategy and method for global profiling of K$_{hib}$ in *P. mirabilis*. *B,* Statistics analysis of the K$_{hib}$ protein, peptides and sites for control (non-enrichment) and experimental group (enrichment). *C,* Identified 2-hydroxyisobutyrylated proteins in all proteins. *D,* The frequency of K$_{hib}$ occurs on proteins.

5′-CTAACTCTATCCTGATCACATTCAACCAA-3′, K343T-antisense: 5′-GTGATCAGGAT AGAGTTAGCAATACCTTT-3′, K343R-sense: 5′-CTAACTCTATCCTGATCAGATTCAAC CAA-3′, K343R-antisense: 5′-CTGATCAGGA TAGAGTTAGCAATACCTTT-3′. *E. coli* BL21 (DE3)/pET28a-ENO, *E. coli* BL21 (DE3)/pET28a-ENO-K343T, and *E. coli* BL21 (DE3)/pET28a-ENO-K343R were grown in 5 ml LB medium containing ampicillin (50 μg/ml) overnight at 37 °C in shaking flasks, and then the cultures were transformed into 500 ml fresh LB medium with ampicillin (50 μg/ml) at 37 °C in shaking flasks to optical density at 600 nm of 0.6–0.8. Cells were induced with 0.15 mM of IPTG at 37 °C for 4 h. The proteins were harvested from cultured cells by lysis buffer (20 mM Tris-HCl, pH 8.0, 10 mM MgCl$_2$, 1 mg/ml lysozyme, 50 U/ml nuclease). Then the proteins were mixed with HisPur Ni-NTA Resin and washed by wash buffer (20 mM Na$_3$Po$_4$, 300 mM NaCl, 25 mM imidazole, pH 7.4), the overexpressed proteins were eluted with elution buffer (20 mM Na$_3$PO$_4$, 300 mM NaCl, 250 mM imidazole, PH 7.4). The elution was collected and concentrated using an Amicon Ultra-0.5 Centrifugal Filter Device in storage buffer (100 mM HEPEs, 10 mM MgCl$_2$, KCl 7.7 mM, pH 7.0).

ENO Activity Assay—The activity of purified ENO, ENO-K343T and ENO-K343R were measured as described (33).

Briefly, the purified proteins were added in the reaction buffer (100 mM HEPEs, 10 mM MgCl$_2$, KCl 7.7 mM, 8 mM 2PG, pH 7.0), and samples without protein served as a blank, after preincubated at 37 °C for 5 min, the reactions were measured at 240 nm on a spectrophotometer to detect the production of phosphoenolpyruvate.

RESULTS AND DISCUSSION

Detection of K$_{hib}$ in P. mirabilis and Verification of Evolutionary Conservatism—K$_{hib}$ was identified in histone proteins from HeLa cells and *Saccharomyces cerevisiae* (24, 26). However, it remains unclear whether the novel PTM exist in other organisms. Toward this goal, we first performed a detection of K$_{hib}$ in *P. mirabilis*. To examine the abundance and distribution of K$_{hib}$ in *P. mirabilis*, we used anti-acetyl lysine (K$_{ac}$) antibody and anti-2-hydroxyisobutyryl lysine antibody to perform the Western blot assay. As shown in Fig. 1*A*–1*D*, a number of 2-hydroxyisobutyrylated proteins are detected. Compared with K$_{ac}$, K$_{hib}$ is also widely distributed and more enriched in 40–70 KDa. The result confirmed the existence of K$_{hib}$ in *P. mirabilis*. To test the evolutionary conservatism of the modification, we further carried out Western blot analysis using the anti-2-hydroxyisobutyryl lysine antibody to
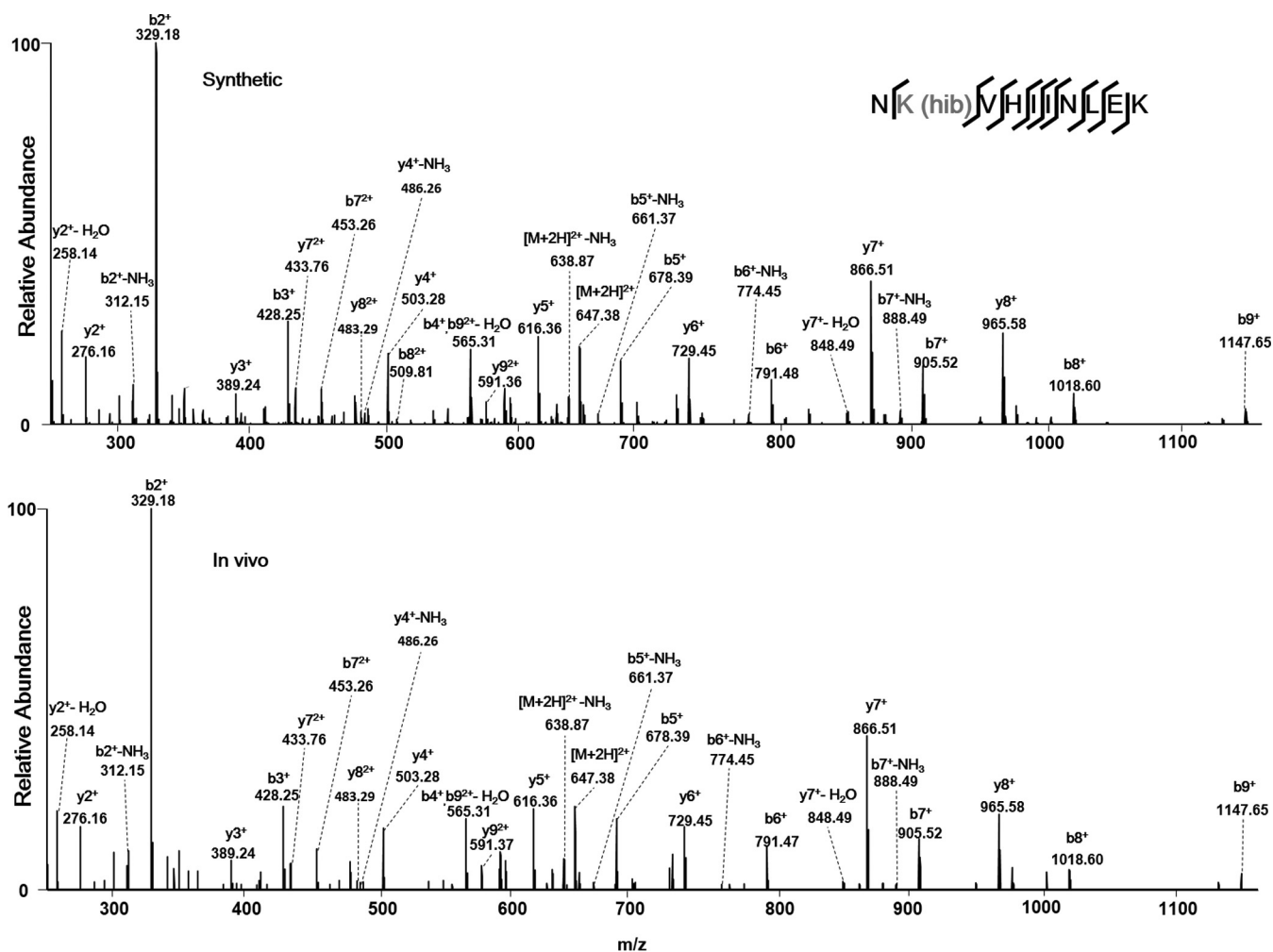
FIG. 3. **The MS/MS spectra of an *in vivo* tryptic peptide bearing** K_{hib} **and its counterpart synthetic peptide.** *A*, MS/MS spectrum of *in vivo* NK$_{hib}$VHIINLEK. *B*, MS/MS spectrum of synthetic NK$_{hib}$VHIINLEK.

other species including *E. coli* (K-12 MG1655), *Saccharomyces cerevisiae* (strain BJ5464 - npga), *Drosophila melanogaster* (S2 cells), *Mus musculus* (C2C12), and human cells (HeLa cells) (Fig. 1*E*). The result showed that K_{hib} is evolutionarily conserved and widely distributed in a variety of organisms.

Analysis Strategy and Identification of Lysine 2-hydroxyisobutyrylated Proteins in P. mirabilis—As a new PTM, K_{hib} was only reported in eukaryotes. It is remarkable that the Western blot assay suggests the existence of K_{hib} in *P. mirabilis*. To further identify potential modified proteins and sites, we performed the PTM analysis using a HPLC-MS/MS. However, we only found 2 peptides bearing the lysine mass shift as same as K_{hib} (supplemental Table S1), which indicated that the PTM is very low in stoichiometry, although it may be widely distributed. To obtain a large scale of K_{hib} proteins and sites in *P. mirabilis*, we performed a systematic analysis of K_{hib} by combining the affinity enrichment and proteomics technique. The method covers 5 steps (Fig. 2*A*): (1) harvest and digestion of the protein lysate of *P. mirabilis*; (2) fraction of

tryptic peptides by HPLC; (3) affinity enrichment of lysine 2-hydroxyisobutyrylated peptides; (4) identification of 2-hydroxyisobutyrylated peptides by LC-MS/MS; (5) finally, characterization and annotation of the modified proteins.

Using this approach, we identified 4724 2-hydroxyisobutyrylated peptides that signified 4735 modified sites on 1051 proteins with less than 1% FDR using MaxQuant software (Fig. 2*B* and supplemental Table S2). In above database, identified 2-hydroxyisobutyrylated peptides with MaxQuant score below than 50, localization probability < 0.75, and PEP > 0.001 had been excluded. To validate the reliability of these modified peptides identified, we synthesized 9 K_{hib} peptides with different lengths and MaxQuant score from 50 to 300. All the MS/MS spectrum of synthetic peptides bearing K_{hib} overlapped almost completely with *in vivo* modified peptides (annotated MS/MS spectra in Fig. 3 and supplemental Fig. S1). The data demonstrated that our approach is highly sensitive for this PTM analysis, meanwhile it revealed many K_{hib} substrates (about 30% proteins were identified to be 2-hydroxyisobutyrulated in *P. mirabilis*, as shown in Fig. 2*C*).
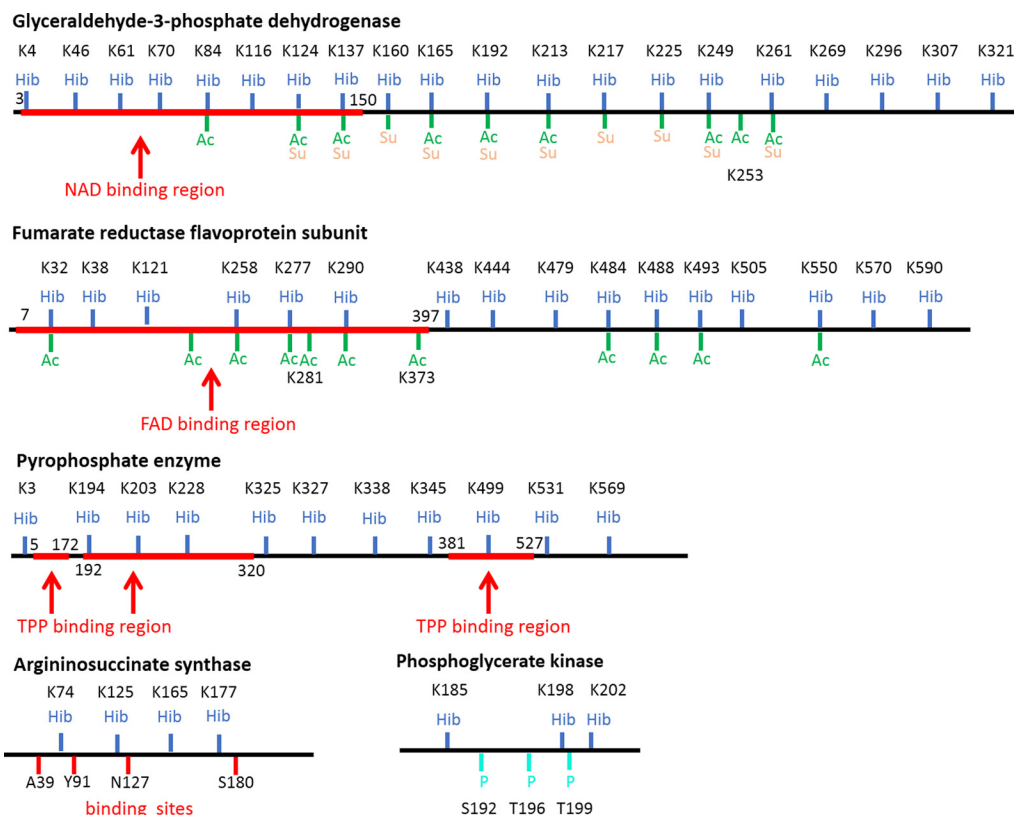
FIG. 4. **Localization of K_{hib} sites in *P. mirabilis*. K_{ac} and K_{succ} were detected in *P. mirabilis* (supplemental Table S3), P was from homologous proteins in *E. coli*. Ac, acetylation; Su, succinylation; P, phosphorylation**.

We further analyzed the frequency of K_{hib} in proteins. In view of all the 2-hydroxyisobutyrylated proteins, 68.8% had 1–5 K_{hib} sites, 19.3% had 6–10 K_{hib} sites, 6.3% had 11–15 K_{hib} sites, and 5.6% had over 15 K_{hib} sites (Fig. 2D). It can be seen from Fig. 2 that the K_{hib} is a multiple and complex PTM in *P. mirabilis*.

Analysis of Lysine 2-hydroxyisobutyrylated Sites—We observed that K_{hib} occurs at key functional regions of proteins in *P. mirabilis*. For example, urease accessory protein (UreE involved in the infection) was 2-hydroxyisobutyrylated on K12 and K21 that locate in the active domain. So, we further analyzed the localization of K_{hib}. While reviewing a previous report, there is no specific description on PTM in *P. mirabilis*. Because *E. coli* has high homology with *P. mirabilis*, we chose the conserved PTM sites as references (34). Fig. 4 indicates that K_{hib} is most likely to possess potential biological functions, it can be demonstrated by the following aspects: 1) K_{hib} shares the same lysine sites with other lysine modifications. For example, K_{hib} shared 7 lysine sites with K_{ac} and 10 lysine sites with K_{succ} in glyceraldehyde-3-phosphate dehydrogenase (these PTMs were identified as shown in supplemental Table S3). Recent work showed that different PTMs at the same lysine may have potential functional cross-talk. For example, the dynamic competition of histone H4K5 and K8 between acetylation and butyrylation is involved in the activation of gene promoters (35). Although the functions of these

K_{hib} sites are unclear now, it is potentially possible that the K_{hib} compete with other PTMs at the same lysine sites. 2) K_{hib} is situated in other PTMs nearby locations. For examples, two 2-hydroxyisobutyrylated sites (K198 and K202) of phosphoglycerate kinase were close to two phosphorylated sites (T196 and T199). It is possible that neighboring modification sites have a reciprocally functional effect. 3) K_{hib} occupied the functional regions. For example, 8 K_{hib} sites occurred in the NAD binding region of glyceraldehyde-3-phosphate dehydrogenase, and 6 K_{hib} sites occurred in FAD binding region of fumarate reductase flavoprotein subunit. Furthermore, 4 K_{hib} sites are located in TPP binding domains of pyrophosphate enzyme. Because K_{hib} can alter charge and hydrophobicity of lysine residue, it is potentially possible that the novel modification plays an important role if localized at some important positions.

Functional Annotation of 2-hydroxyisobutyrylated Proteins—To better understand the potential function of K_{hib}, we performed functional annotation analysis via the Gene Ontology (GO) tool. First, we investigated the GO functional classification of all the 2-hydroxyisobutyrylated proteins based on their biological process, cellular component, and molecular function. As shown in Fig. 5, most of the 2-hydroxyisobutyrylated proteins were enriched in translation, cell division, proteolysis, and tricarboxylic acid cycle (Fig. 5). Interestingly, most of the 2-hydroxyisobutyrylated proteins were related to
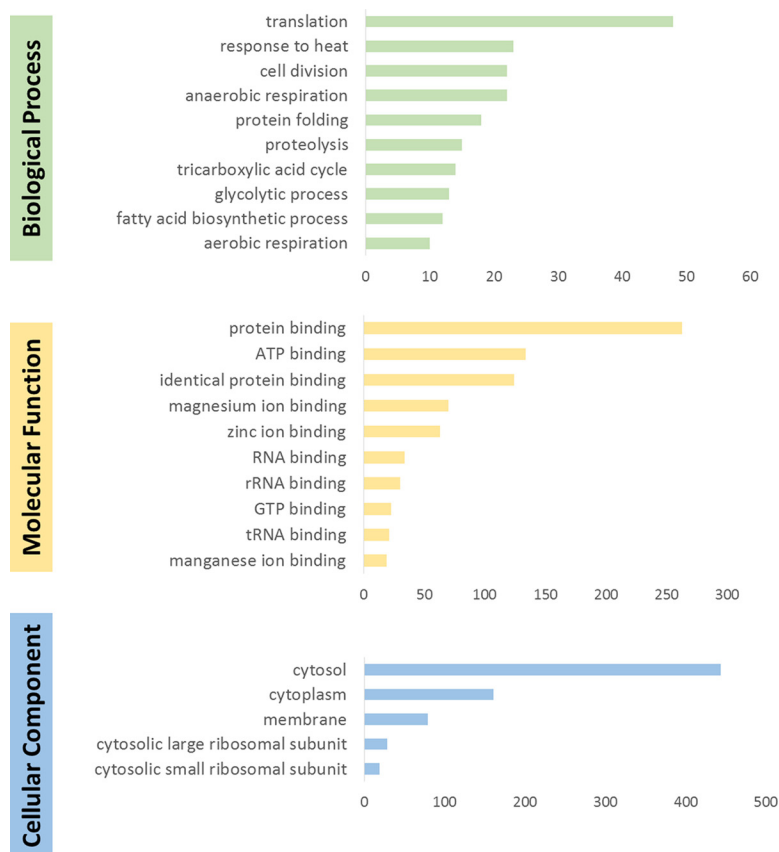
FIG. 5. **Analysis the biological process, molecular function and cellular component of 2-hydroxyisobutyrylated proteins in *P. mirabilis*.**
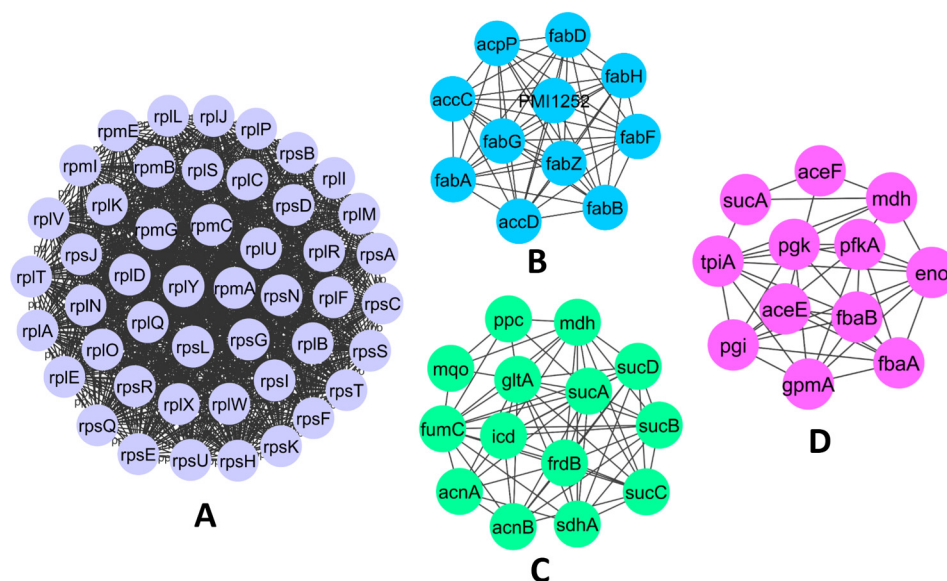
FIG. 6. **Interaction networks of 2-hydroxyisobutyrylated proteins in *P. mirabilis*.** *A*, 48 ribosome-associated proteins. *B*, 12 2-hydroxy-isobutyrylated proteins associated with fatty acid biosynthetic process. *C*, 14 proteins associated with TCA. *D*, 13 2-hydroxyisobutyrylated proteins associated with glucolysis.

the various binding targets and metabolism. Assortment of cellular components showed that 58.4% of the 2-hydroxy-isobutyrylated proteins were in the cytosol, 10.4% in the membrane, and 6.3% in the ribosomal subunit. Most of the modified proteins that appeared on the cytosol and cell membrane suggested that K_{hib} may play a key role in cell structure and regulate the intracellular life process such as translation and metabolism in *P. mirabilis*.

INTERPRO
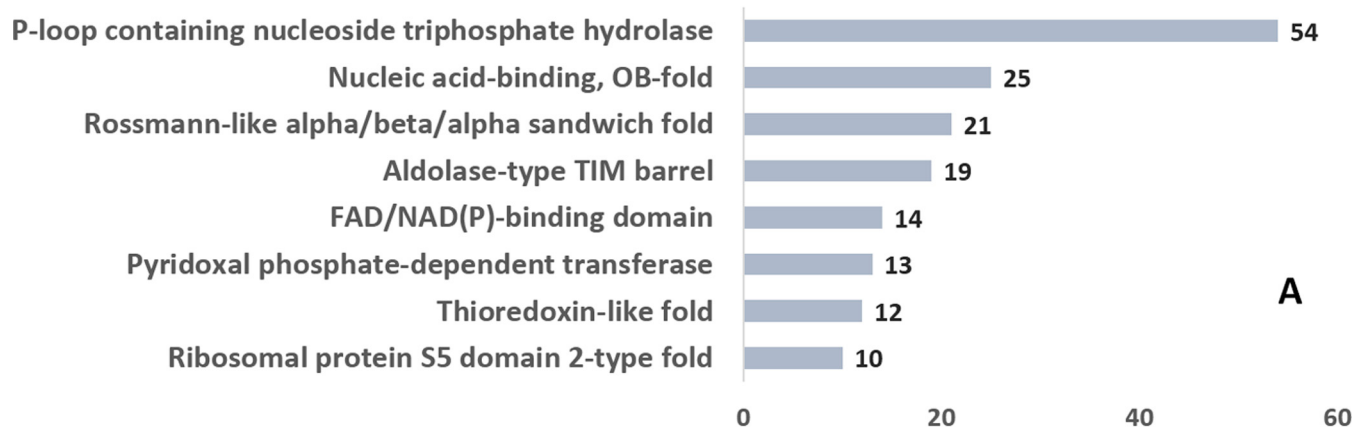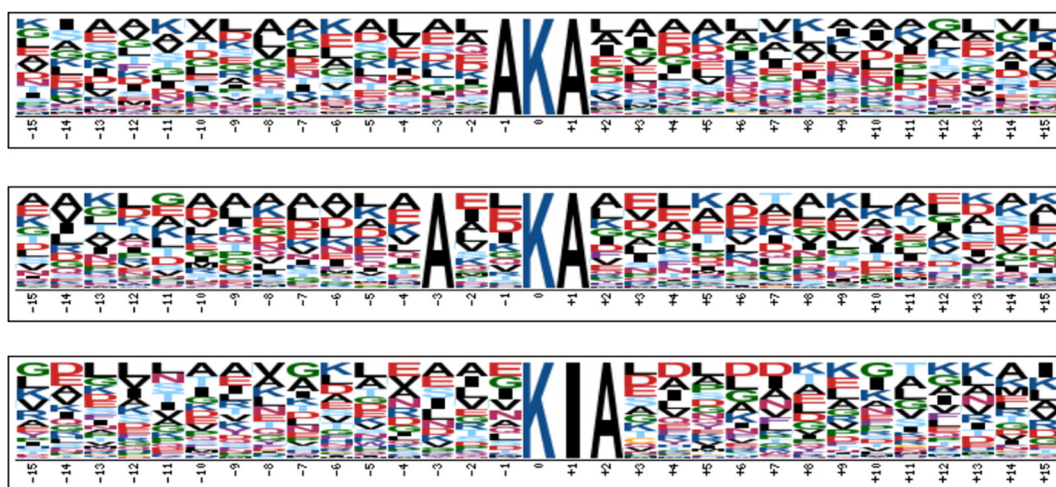
Motif-X

FIG. 7. **Characterization of the domains and sequence Recognition Motifs.** *A,* Statistics of the various domains of 2-hydroxyisobutyry-lated proteins in *P. mirabilis*. *B,* Sequence Logo representation of significant motifs identified by Motif-X software. The motifs with significance of $p < 0.000001$ are shown. The motifs take 2-hydroxyisobutyrylated lysine as center and show the distribution of 15 amino acids in both sides in *P. mirabilis*.

Interaction Networks of 2-hydroxyisobutyrylated Pro-teins—To further investigate the correlation of 2-hydroxy-isobutyrylated proteins in *P. mirabilis*, we performed the pro-tein-protein interaction networks via STRING and Cytoscape. Our results showed that 743 of the 2-hydroxyisobutyrylated proteins were closely connected. So, we further analyzed subgroups according to their functions. For example, 48 ri-bosome-associated proteins and 12 proteins associated with fatty acid biosynthetic process had been analyzed to evaluate their connections, respectively, and their interaction networks are close (Fig. 6), which is similar with the interaction networks of acetylated proteins (4). It also indicated that K_{hib} is relatively active in multiple biological processes in *P. mirabilis*.

Characterization of the Domains and Sequence Recognition Motifs—We further studied the structural properties of the 2-hydroxyisobutyrylated proteins through DAVID INTERPRO.

And we found that p-loop containing nucleoside triphosphate hydrolase, nucleic acid-binding, rossmann-like alpha/beta/alpha sandwich fold and aldolase-type TIM barrel were the main domains in these modified proteins (Fig. 7A). We also analyzed the position-specific amino acid frequency of the surrounding sequences (15 amino acids to both termini) of 2-hydroxyisobutyrylated lysine residues using Motif-X. It can be seen from Fig. 7B that alanine was drastically overrepre-sented in +1, +2, −1 and −3 positions. In addition, the sequence signatures "AKA," "AXXKA," and "KIA" were pre-ferred in the peptides bearing K_{hib}. It indicates that lysine in these locations was likely to occur K_{hib} in *P. mirabilis*.

2-hydroxyisobutyrylation of Enzymes Involved in Central Metabolism—Many metabolic enzymes were detected to be 2-hydroxyisobutyrylated (supplemental Table S4), so we fo-cused on the analysis of 2-hydroxyisobutyrylated proteins in

FIG. 8. **The 2-hydroxyisobutyrylated enzymes in central carbon metabolism network in *P. mirabilis*.** The identified 2-hydroxyisobutyrylated proteins were colored.

metabolic pathways. As described in Fig. 8, a large proportion of metabolic enzymes are 2-hydroxyisobutyrylated in pentose phosphate pathway, TCA cycle and glycolysis/gluconeogenesis. It is unexpected that 54 crucial enzymes were 2-hydroxyisobutyrylated in total of the three pathways, and 26% of them had more than ten 2-hydroxyisobutyrylated sites. The result raises some interesting questions. Why and how these enzymes are highly 2-hydroxyisobutyrylated? What role does 2-hydroxyisobutyrylat play in the regulation of metabolic enzymes structure and function? Are these modifications regulated by carbon sources in metabolic pathways?

Regulation of Lysine 2-hydroxyisobutyrylation by Carbon Sources in Metabolism—Recent report suggested that K_{hib} is most likely generated via 2-hydroxyisobutyryl-CoA (HibCoA) as a cofactor (24). It has been known that HibCoA can be regulated by carbon sources in bacteria (36). So we further investigated the influence of different carbon sources on 2-hydroxyisobutyrylation statues. The abundance of K_{hib} was investigated in *P. mirabilis* grown in M9 medium without an additional carbon source or treated with 0.8% glucose, 0.8% pyruvate and 0.8% 2-HIBA, respectively. Western blotting assay showed that *P. mirabilis* with glucose, pyruvate or 2-HIBA were significantly 2-hydroxyisobutyrylated, compared with that in M9 medium (Fig. 9A and 9B). The result demonstrated that K_{hib} was dependent on carbon sources in *P. mirabilis.* Interestingly, the same concentration of metabolic fuels had different effect on the modification. The carbon sources of glucose, pyruvate and 2-HIBA caused the 2-hy-

droxyisobutyrylation increased in turn (Fig. 9B). To illustrate the different regulation of three carbon sources, we further investigated their relationship with HibCoA in metabolic pathways in *P. mirabilis* (Fig. 9C). 2-HIBA may generate HibCoA directly, whereas, glucose and pyruvate need several additional steps to generate HibCoA, moreover they can be used by metabolic bypasses, and therefore it can be concluded that the different positions of carbon sources in metabolism may determine the regulation capacity for K_{hib} in *P. mirabilis*. These results suggested that K_{hib} may mediate adaptation to various carbon sources in *P. mirabilis,* meanwhile the modification may be associated with metabolic regulation.

Simulation of Substrate and Enzyme Docking—Recent study demonstrated that lysine modifications such succinylation and malonylation suppressed enzymatic activity (15, 37). In this study, we identified much K_{hib} on metabolic enzymes, and therefore we would like to know if the modification has a potential effect on their activities too? Because the binding between enzyme and its substrate is a crucial step in the process, we employed molecular docking to generate the binding conformation of small molecule (substrate) into the enzyme structure with and without K_{hib} and to probe the likely effect of K_{hib} on enzymatic activity. Enolase (ENO) is a key enzyme in glucolysis and gluconeogenesis that catalyzes 2PG to phosphoenolpyruvate (the active sites and the substrate binding sites of enzymes in supplemental Table S5, and the structures of the enzyme and substrate in supplemental Fig. S2). As shown in Fig. 10A, the identified K_{hib} site (K343) in

Fig. 9. **Anti-lysine 2-hydroxyisobutyrylation immunoblots showing that different carbon sources altered 2-hydroxyisobutyrylation of *P. mirabilis*.** *A,* Coomassie blue staining of protein lysates from different carbon sources (0.8% glucose, 0.8% pyruvate, 0.8% 2-HIBA) of cultures was used for the loading control. *B*, Western blotting analysis of lysine succinylation level in protein lysates from different carbon sources (0.8% glucose, 0.8% pyruvate, 0.8% 2-HIBA) of cultures with a pan anti-2-hydroxy-isobutyryllysine antibody. *C*, The metabolic pathway of ingested glucose, pyruvate and 2-HIBA in *P. mirabilis*.

ENO was used to dock the substrate, 2PG. Fig. 10*A* shows that 2PG binds to two different pockets pending on the modification. In the absence of K_{hib}, 2PG binds to the substrate binding site that is consisted of S42, K343, R372, and S373. In contrast, in the presence of K_{hib}, it binds to the neighboring site that is composed of G40, A41, S42, S187, and D318. Meanwhile, the binding energy is reduced from −3.31 kcal/mol to −2.34 kcal/mol and the distances between 2PG and two key residues for enzymatic activity, E209 and K343, are significantly increased from 4.482 Å to 12.005 Å and from 3.044 Å to 11.008 Å, respectively. Based on these data, it is tempting to speculate that the K_{hib} (K343) may destroy the environment of binding sites in ENO, and consequently the substrate is not properly positioned within the binding site, which may eventually influence the enzymatic activity of ENO.

Confirmation the Effect of 2-hydroxyisobutyrylation on ENO Activity—To verify the docking result, we locked 2-hydroxy-isobutyrylated K343 of ENO by T and non-2-hydroxyisobu-tyrylated K343 of ENO by R. We cloned, overexpressed and purified ENO (ENO-K343T and ENO-K343R) of *P. mirabilis* as a His-tagged fusion protein. The purified proteins were verified by DNA sequence blast and MS analysis (supplemental Fig. S3). Based on the conservation analysis, K343 of ENO were conserved in the orthologs of *P. mirabilis,* also indicating K343 might be important for an evolutionarily conserved function (Fig. 11*A*). Using the unmodified BSA as control, the

Fig. 10. **Using AutoDock to simulate the binding conformation of ENO with its substrate 2-phosphoᴅglycerate.** Binding conformation of ENO with 2-phospho-ᴅ-glycerate with and without 2-hydroxisobutyrylation of K343. E209 and K343 are the active sites of ENO, the position of green 2PG represents the binding location without Khib (K343), the position of red 2PG represents the binding location with Khib (K343), pocket A shows the substrate binding region without Khib, pocket B shows the substrate binding region with Khib, the rad box show the distance between ENO and 2PG.

Fig. 11. **Amino acid mutation of ENO from *P. mirabilis*.** (A) Multiple sequence alignment of ENO from different species. The conserved K343 site were marked by the black arrow. (B) The 2-hydroxyisobutyrylation levels of purified recombinant ENO were determined by Western blot using 2-hydroxyisobutyrylated lysine antibodies. (C) 2-hydroxyisobutyrylation on K343 affect the enzyme activity of ENO. Detection the activity of ENO and its mutants (K343T, K343R) (data are means±S.D. from three independent assays, **: $p < 0.05$, ***: $p < 0.001$).

Western blot illustrated recombinant ENO was 2-hydroxyisobutyrylated and unmodified BSA was not detected (Fig. 11*B*). Then we measured the enzymatic activity of ENO and its mutants. The results showed that mutation of K343 to R, which conserved the positive charge and locked as unmodified lysine, led to a significant increase of the enzymatic activity compared with ENO, but mutation of K343 to T, which locked as 2-hydroxyisobutyrylated lysine, led to a decrease in

the enzymatic activity (Fig. 11C). In line with the docking result, these data suggest that 2-hydroxyisobutyrylation on K343 was a negative regulatory modification on ENO activity.

Conclusions and Perspectives—In this study, we combined high affinity enrichment with mass spectrometry analysis and bioinformatics tools for the first comprehensive analysis of K_{hib} in *P. mirabilis*. Totally we identified 4735 lysine 2-hydroxyisobutyrylation sites in 1051 proteins. Our result demonstrated that the combined approach is powerful for identification and characterization of K_{hib} on a large scale. And we also demonstrated that central metabolism enzymes in *P. mirabilis* were 2-hydroxyisobutyrylated extensively. Furthermore, we showed that 2-hydroxyisobutyrylation on K343 was a negative regulatory modification on ENO activity, and molecular docking results indicate the regulatory mechanism that K_{hib} may change the binding formation of ENO and its substrate 2PG and cause the substrate far from the active sites of enzyme, consequently, the catalytic activity of the enzymes might be affected. Meanwhile, the concerted changes in K_{hib} dependent on carbon source revealed that K_{hib} may mediate adaptation to various carbon sources, and indicated that K_{hib} is of potential significance to metabolic regulation. This work represents a significant expansion of our current understanding of K_{hib} and provides foundation for further studying biological functions of this modification.

DATA AVAILABILITY

The mass spectrometry proteomics data (raw data and search results files generated by MaxQuant) have been deposited at iProX with the data set identifier IPX0000942000 (downloaded free from http://www.iprox.org/page/PDV014. html?projectId=IPX0000942000) and the annotated spectra can be obtained at MS-Viewer (search keys: abmvlxmqks and rupesblkbg) (http://msviewer.ucsf.edu/prospector/cgi-bin/msform.cgi?form=msviewer).

¶¶ To whom correspondence should be addressed: 2011 Collaborative Innovation Center of Tianjin for Medical Epigenetics, Tianjin Key Laboratory of Medical Epigenetics, Department of Biochemistry and Molecular Biology, Tianjin Medical University, Tianjin 300070, China. E-mail: kzhang@tmu.edu.cn.

REFERENCES

1. Jensen, O. N. (2006) Interpreting the protein language using proteomics. *Nat. Rev. Mol. Cell Bio.* **7,** 391–403
2. Huang, H., Sabari, B. R., Garcia, B. A., Allis, C. D., and Zhao, Y. (2014) SnapShot: histone modifications. *Cell* **159,** 458–458.e1
3. Kim, S. C., Sprung, R., Chen, Y., Xu, Y., Ball, H., Pei, J., Cheng, T., Kho, Y., Xiao, H., Xiao, L., Grishin, N. V., White, M., Yang, X. J., and Zhao, Y. (2006) Substrate and functional diversity of lysine acetylation revealed by a proteomics survey. *Mol. Cell* **23,** 607–618
4. Choudhary, C., Kumar, C., Gnad, F., Nielsen, M. L., Rehman, M., Walther, T. C., Olsen, J. V., and Mann, M. (2009) Lysine acetylation targets protein complexes and co-regulates major cellular functions. *Science* **325,** 834–840
5. Zhao, S. M., Xu, W., Jiang, W. Q., Yu, W., Lin, Y., Zhang, T. F., Yao, J., Zhou, L., Zeng, Y. X., Li, H., Li, Y. X., Shi, J., An, W. L., Hancock, S. M., He, F. C., Qin, L. X., Chin, J., Yang, P. Y., Chen, X., Lei, Q. Y., Xiong, Y., and Guan, K. L. (2010) Regulation of cellular metabolism by protein lysine acetylation. *Science* **327,** 1000–1004
6. Chen, Y., Zhao, W. H., Yang, J. S., Cheng, Z. Y., Luo, H., Lu, Z. K., Tan, M. J., Gu, W., and Zhao, Y. M. (2012) Quantitative acetylome analysis reveals the roles of sirt1 in regulating diverse substrates and cellular pathways. *Mol. Cell. Proteomics* **11,** 1048–1062
7. Weinert, B. T., Scholz, C., Wagner, S. A., Iesmantavicius, V., Su, D., Daniel, J. A., and Choudhary, C. (2013) Lysine succinylation is a frequently occurring modification in prokaryotes and eukaryotes and extensively overlaps with acetylation. *Cell Rep.* **4,** 842–851
8. Sabari, B. R., Zhang, D., Allis, C. D., and Zhao, Y. M. (2017) Metabolic regulation of gene expression through histone acylations. *Nat. Rev. Mol. Cell Bio.* **18,** 90–101
9. Zhang, Y. Y., Fonslow, B. R., Shan, B., Baek, M. C., and Yates, J. R. (2013) Protein analysis by shotgun/bottom-up proteomics. *Chem. Rev.* **113,** 2343–2394
10. Huang, H., Lin, S., Garcia, B. A., and Zhao, Y. M. (2015) Quantitative proteomic analysis of histone modifications. *Chem. Rev.* **115,** 2376–2418
11. Zhang, Z., Tan, M., Xie, Z., Dai, L., Chen, Y., and Zhao, Y. (2011) Identification of lysine succinylation as a new post-translational modification. *Nat. Chem. Biol.* **7,** 58–63
12. Xie, Z. Y., Dai, J. B. A., Dai, L. Z., Tan, M. J., Cheng, Z. Y., Wu, Y. M., Boeke, J. D., and Zhao, Y. M. (2012) Lysine succinylation and lysine malonylation in histones. *Mol. Cell. Proteomics* **11,** 100–107
13. Colak, G., Xie, Z. Y., Zhu, A. Y., Dai, L. Z., Lu, Z. K., Zhang, Y., Wan, X. L., Chen, Y., Cha, Y. H., Lin, H. N., Zhao, Y. M., and Tan, M. J. (2013) Identification of lysine succinylation substrates and the succinylation regulatory enzyme CobB in Escherichia coli. *Mol. Cell. Proteomics* **12,** 3509–3520
14. Rardin, M. J., He, W. J., Nishida, Y., Newman, J. C., Carrico, C., Danielson, S. R., Guo, A., Gut, P., Sahu, A. K., Li, B., Uppala, R., Fitch, M., Riiff, T., Zhu, L., Zhou, J., Mulhern, D., Stevens, R. D., Ilkayeva, O. R., Newgard, C. B., Jacobson, M. P., Hellerstein, M., Goetzman, E. S., Gibson, B. W., and Verdin, E. (2013) SIRT5 Regulates the mitochondrial lysine succinylome and metabolic networks. *Cell Metab.* **18,** 920–933
15. Yang, M. K., Wang, Y., Chen, Y., Cheng, Z. Y., Gu, J., Deng, J. Y., Bi, L. J., Chen, C. B., Mo, R., Wang, X. D., and Ge, F. (2015) Succinylome analysis reveals the involvement of lysine succinylation in metabolism in pathogenic mycobacterium tuberculosis. *Mol. Cell. Proteomics* **14,** 796–811
16. Tan, M. J., Luo, H., Lee, S., Jin, F. L., Yang, J. S., Montellier, E., Buchou, T., Cheng, Z. Y., Rousseaux, S., Rajagopal, N., Lu, Z. K., Ye, Z., Zhu, Q., Wysocka, J., Ye, Y., Khochbin, S., Ren, B., and Zhao, Y. M. (2011) Identification of 67 histone marks and histone lysine crotonylation as a new type of histone modification. *Cell* **146,** 1015–1027
17. Montellier, E., Rousseaux, S., Zhao, Y. M., and Khochbin, S. (2012) Histone crotonylation specifically marks the haploid male germ cell gene expression program. *Bioessays* **34,** 187–193
18. Sabari, B. R., Tang, Z. Y., Huang, H., Yong-Gonzalez, V., Molina, H., Kong, H. E., Dai, L. Z., Shimada, M., Cross, J. R., Zhao, Y. M., Roeder, R. G., and Allis, C. D. (2015) Intracellular crotonyl-CoA stimulates transcription through p300-catalyzed histone crotonylation. *Mol. Cell* **58,** 203–215
19. Li, Y. Y., Sabari, B. R., Panchenko, T., Wen, H., Zhao, D., Guan, H. P., Wan, L. L., Huang, H., Tang, Z. Y., Zhao, Y. M., Roeder, R. G., Shi, X. B., Allis, C. D., and Li, H. T. (2016) Molecular coupling of histone crotonylation and active transcription by AF9 YEATS domain. *Mol. Cell* **62,** 181–193
20. Peng, C., Lu, Z. K., Xie, Z. Y., Cheng, Z. Y., Chen, Y., Tan, M. J., Luo, H., Zhang, Y., He, W., Yang, K., Zwaans, B. M. M., Tishkoff, D., Ho, L., Lombard, D., He, T. C., Dai, J. B., Verdin, E., Ye, Y., and Zhao, Y. M. (2011) The first identification of lysine malonylation substrates and its regulatory enzyme. *Mol. Cell. Proteomics* **10,** M111.012658
21. Hirschey, M. D., and Zhao, Y. M. (2015) Metabolic regulation by lysine malonylation, succinylation, and glutarylation. *Mol. Cell. Proteomics* **14,** 2308–2315
22. Tan, M. J., Peng, C., Anderson, K. A., Chhoy, P., Xie, Z. Y., Dai, L. Z., Park, J., Chen, Y., Huang, H., Zhang, Y., Ro, J., Wagner, G. R., Green, M. F.,

Madsen, A. S., Schmiesing, J., Peterson, B. S., Xu, G. F., Ilkayeva, O. R., Muehlbauer, M. J., Braulke, T., Muhlhausen, C., Backos, D. S., Olsen, C. A., McGuire, P. J., Pletcher, S. D., Lombard, D. B., Hirschey, M. D., and Zhao, Y. M. (2014) Lysine glutarylation is a protein posttranslational modification regulated by SIRT5. *Cell Metabolism* **19,** 605–617

23. Xie, L. X., Wang, G. R., Yu, Z. X., Zhou, M. L., Li, Q. M., Huang, H. R., and Xie, J. P. (2016) Proteome-wide lysine glutarylation profiling of the mycobacterium tuberculosis H37Rv. *J. Proteome Res.* **15,** 1379–1385

24. Dai, L. Z., Peng, C., Montellier, E., Lu, Z. K., Chen, Y., Ishii, H., Debernardi, A., Buchou, T., Rousseaux, S., Jin, F. L., Sabari, B. R., Deng, Z. Y., Allis, C. D., Ren, B., Khochbin, S., and Zhao, Y. M. (2014) Lysine 2-hydroxyisobutyrylation is a widely distributed active histone mark. *Nat. Chem. Biol.* **10,** U365–U373

25. Rousseaux, S., and Khochbin, S. (2015) Histone acylation beyond acetylation: terra incognita in chromatin biology. *Cell J.* **17,** 1–6

26. Huang, J., Luo, Z. Q., Ying, W. T., Cao, Q. C., Huang, H., Dong, J. K., Wu, Q. Y., Zhao, Y. M., Qian, X. H., and Dai, J. B. (2017) 2-Hydroxyisobutyrylation on histone H4K8 is regulated by glucose homeostasis in Saccharomyces cerevisiae. *Proc. Natl. Acad. Sci. U.S.A.* **114,** 8782–8787

27. Zhang, K., Zheng, S. Z., Yang, J. S., Chen, Y., and Cheng, Z. Y. (2013) Comprehensive profiling of protein lysine acetylation in Escherichia coli. *J. Proteome Res.* **12,** 844–851

28. Morris, G. M., Huey, R., Lindstrom, W., Sanner, M. F., Belew, R. K., Goodsell, D. S., and Olson, A. J. (2009) AutoDock4 and AutoDockTools4: Automated docking with selective receptor flexibility. *J. Comput. Chem.* **30,** 2785–2791

29. Biasini, M., Bienert, S., Waterhouse, A., Arnold, K., Studer, G., Schmidt, T., Kiefer, F., Cassarino, T. G., Bertoni, M., Bordoli, L., and Schwede, T. (2014) SWISS-MODEL: modelling protein tertiary and quaternary structure using evolutionary information. *Nucleic Acids Res.* **42,** W252–W258

30. Pettersen, E. F., Goddard, T. D., Huang, C. C., Couch, G. S., Greenblatt, D. M., Meng, E. C., and Ferrin, T. E. (2004) UCSF chimera - A visualization system for exploratory research and analysis. *J. Comput. Chem.* **25,** 1605–1612

31. Law, V., Knox, C., Djoumbou, Y., Jewison, T., Guo, A. C., Liu, Y., Maciejewski, A., Arndt, D., Wilson, M., Neveu, V., Tang, A., Gabriel, G., Ly, C., Adamjee, S., Dame, Z. T., Han, B., Zhou, Y., and Wishart, D. S. (2014) DrugBank 4.0: shedding new light on drug metabolism. *Nucleic Acids Res.* **42,** D1091–D1097

32. Bateman, A., Martin, M. J., O'Donovan, C., Magrane, M., Alpi, E., Antunes, R., Bely, B., Bingley, M., Bonilla, C., Britto, R., Bursteinas, B., Bye Jee, -A. -H., Cowley, A., Da Silva, A., De Giorgi, M., Dogan, T., Fazzini, F., Castro, L. G., Figueira, L., Garmiri, P., Georghiou, G., Gonzalez, D., Hatton-Ellis, E., Li, W. Z., Liu, W. D., Lopez, R., Luo, J., Lussi, Y., MacDougall, A., Nightingale, A., Palka, B., Pichler, K., Poggioli, D., Pundir, S., Pureza, L., Qi, G. Y., Rosanoff, S., Saidi, R., Sawford, T., Shypitsyna, A., Speretta, E., Turner, E., Tyagi, N., Volynkin, V., Wardell, T., Warner, K., Watkins, X., Zaru, R., Zellner, H., Xenarios, I., Bougueleret, L., Bridge, A., Poux, S., Redaschi, N., Aimo, L., Argoud-Puy, G., Auchincloss, A., Axelsen, K., Bansal, P., Baratin, D., Blatter, M. C., Boeckmann, B., Bolleman, J., Boutet, E., Breuza, L., Casal-Casas, C., de Castro, E., Coudert, E., Cuche, B., Doche, M., Dornevil, D., Duvaud, S., Estreicher, A., Famiglietti, L., Feuermann, M., Gasteiger, E., Gehant, S., Gerritsen, V., Gos, A., Gruaz-Gumowski, N., Hinz, U., Hulo, C., Jungo, F., Keller, G., Lara, V., Lemercier, P., Lieberherr, D., Lombardot, T., Martin, X., Masson, P., Morgat, A., Neto, T., Nouspikel, N., Paesano, S., Pedruzzi, I., Pilbout, S., Pozzato, M., Pruess, M., Rivoire, C., Roechert, B., Schneider, M., Sigrist, C., Sonesson, K., Staehli, S., Stutz, A., Sundaram, S., Tognolli, M., Verbregue, L., Veuthey, A. L., Wu, C. H., Arighi, C. N., Arminski, L., Chen, C. M., Chen, Y. X., Garavelli, J. S., Huang, H. Z., Laiho, K., McGarvey, P., Natale, D. A., Ross, K., Vinayaka, C. R., Wang, Q. H., Wang, Y. Q., Yeh, L. S., Zhang, J., and Consortium, U. (2017) UniProt: the universal protein knowledgebase. *Nucleic Acids Res.* **45,** D158–D169

33. Feng, Y. J., Pan, X. Z., Sun, W., Wang, C. J., Zhang, H. M., Li, X. F., Ma, Y., Shao, Z. Q., Ge, J. C., Zheng, F., Gao, G. F., and Tang, J. Q. (2009) Streptococcus suis enolase functions as a protective antigen displayed on the bacterial cell surface. *J. Infectious Dis.* **200,** 1583–1592

34. Macek, B., Gnad, F., Soufi, B., Kumar, C., Olsen, J. V., Mijakovic, I., and Mann, M. (2008) Phosphoproteome analysis of E-coli reveals evolutionary conservation of bacterial Ser/Thr/Tyr phosphorylation. *Mol. Cell. Proteomics* **7,** 299–307

35. Goudarzi, A., Zhang, D., Huang, H., Barral, S., Kwon, O. K., Qi, S. K., Tang, Z. Y., Buchou, T., Vitte, A. L., He, T. M., Cheng, Z. Y., Montellier, E., Gaucher, J., Curtet, S., Debernardi, A., Charbonnier, G., Puthier, D., Petosa, C., Panne, D., Rousseaux, S., Roeder, R. G., Zhao, Y. M., and Khochbin, S. (2016) Dynamic competing histone H4 K5K8 acetylation and butyrylation are hallmarks of highly active gene promoters. *Mol. Cell* **62,** 169–180

36. Rohwerder, T., and Muller, R. H. (2010) Biosynthesis of 2-hydroxyisobutyric acid (2-HIBA) from renewable carbon. *Microb. Cell Fact.* **9,** 13

37. Qian, L. L., Nie, L. T., Chen, M., Liu, P., Zhu, J., Zhai, L. H., Tao, S. C., Cheng, Z. Y., Zhao, Y. M., and Tan, M. J. (2016) Global profiling of protein lysine malonylation in Escherichia coli reveals its role in energy metabolism. *J. Proteome Res.* **15,** 2060–2071

MOLECULAR & CELLULAR PROTEOMICS